

RECENT PROGRESS IN THE DEVELOPMENT OF A STAND-ALONE GERMANIUM SOLAR CELL

N.E. Posthuma, J. van der Heide, G. Flamand and J. Poortmans

IMEC vzw, Kapeldreef 75, B-3001 Leuven, Belgium

Phone: +32-16-28 8178; Fax: +32-16-28 1501, electronic mail: niels.posthuma@imec.be

ABSTRACT: Stand-alone germanium solar cells can be applied in various systems like mechanically stacked high-efficiency multi-junction solar cells, thermo-photovoltaic systems or hybrid lighting systems, since these solar cells have a spectral sensitivity up to a wavelength of 1800 nm. Critical elements in achieving a highly efficient germanium solar cell are the emitter formation, surface passivation and contact formation. The investigated and applied processes contain phosphorous diffusion using spin-on diffusants, surface passivation by PECVD amorphous silicon and contact formation using an innovative process where the contacting metal is diffused through the passivation layer to establish the contact. The developed germanium solar cell process has resulted in world-class energy conversion efficiencies well above 7 percent (AM1.5G, $C=1$ sun). The best realised solar cell ($0.5 \times 0.5 \text{ cm}^2$) has an efficiency of 8.4 percent, with a J_{sc} of 50 mA/cm^2 , a V_{oc} of 258 mV and a fill factor of 65 percent.

Keywords: germanium, contact, diffusion

1 INTRODUCTION

Germanium is a suitable material to realise solar cells with a spectral sensitivity up to 1800 nm. As a stand-alone application the germanium solar cell can be used in thermo-photovoltaic (TPV) or hybrid lighting systems. Alternatively, it can be combined with III-V solar cells to be used in a mechanically stacked high-efficiency multi-junction solar cell. The advantage of this stacking method compared to series connected monolithically stacked cells is relaxation of the current matching requirement. This allows full benefit from the current generated by the germanium bottom cell.




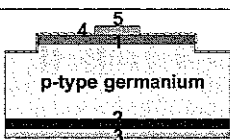
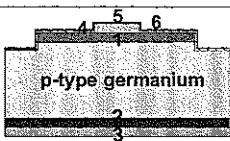
Currently at IMEC, a mechanically stacked high-efficiency solar cell consisting of an InGaP₂/GaAs top cell in combination with a stand-alone germanium bottom cell is under investigation. For this purpose, over the last years a stand-alone germanium solar cell has been developed [1, 2]. Specific attention has been given to the emitter formation, surface passivation and the realisation of front and back side contacts. Recently significant progress has been made in optimising the solar cell process and improving its reproducibility.

In this paper first the germanium solar cell process as it has been developed is described in paragraph 2. The specific details of several important process steps will be discussed separately. In the subsequent paragraph an overview will be given of the solar cell results obtained recently. Finally conclusions are drawn and subjects for further research are described.

2 GERMANIUM SOLAR CELL PROCESS

The developed germanium solar cell process consists of six basic steps [1, 2], which have been studied in detail and will be described below. The starting material of the solar cell process is a 4-inch 145 μm thick p-type germanium substrate with a resistivity of $0.025 \text{ Ohm}\cdot\text{cm}$ ($\sim 1 \cdot 10^{17} \text{ cm}^{-3}$), the front side of the wafer is mirror polished while the back side is ground. An overview of the most important process steps is given in Table I.

Table I: Overview of the main steps of the germanium solar cell process.

#	Description	Illustration
1	1. n ⁺ emitter	
2	1. n ⁺ emitter 2. BSF 3. Back contact	
3	1. n ⁺ emitter 2. BSF 3. Back contact	
4	1. n ⁺ emitter	
5	2. BSF 3. Back contact 4. Passivation layer 5. Front contact	
6	1. n ⁺ emitter 2. BSF 3. Back contact 4. Passivation layer 5. Front contact 6. Double ARC	

2.1 Emitter formation

The first main step of the solar cell process is emitter formation (Table I, step 1), which is done by phosphorous diffusion from a spin-on dopant (SOD) source. Ideally an emitter profile is obtained with a sheet resistivity of 50 to 80 $\text{Ohm}\cdot\text{cm}$, with a surface doping level of around $1 \cdot 10^{19} \text{ cm}^{-3}$. Critical parameters are the diffusion time, diffusion temperature, SOD layer thickness and the SOD phosphorous content. Realised diffusion profiles have been studied by secondary ion mass spectroscopy (SIMS), spreading resistance profiling (SRP) and 4-point probe measurements. In our experiments phosphorous diffusion is done at 550 to 650 °C during several minutes. Most striking is the

influence of the phosphorous concentration in the SOD, as shown in the SIMS curves of Figure 1, where only the SOD type has been varied. An increased diffusion depth is observed for higher phosphorous concentration in the SOD. Due to non-Fickian diffusion, for SODs with a high phosphorous content, the initial rate of diffusion is enhanced, as will be presented in more detail elsewhere [3].

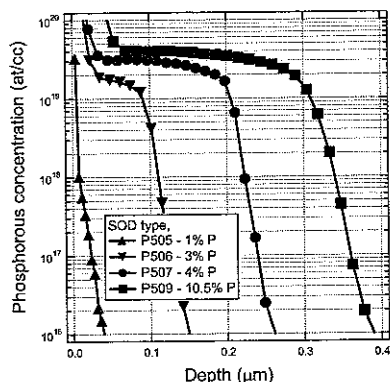


Figure 1: SIMS measurement results for phosphorous diffusion in germanium, with varying phosphorous concentration in the spin-on dopant source. Except the phosphorous concentration in the SOD all the other diffusion parameters have been kept constant.

The SIMS measurements, as shown in Figure 1, show furthermore that a highly doped dead layer is present for most of the obtained profiles. During the solar cell process this dead layer is removed by a wet-chemical treatment in order to achieve better surface passivation.

Furthermore it has been observed that since the used germanium wafers have a thickness of only 145 μm , during spin-coating the wafer slightly bends. As a result, for a thin SOD-layer, a non-uniform sheet resistance distribution is obtained over the wafer area. Application of a thicker SOD-layer results in a more uniform phosphorous distribution, as shown by 4-point probe measurements summarised in Table II. In this experiment, for the two samples all diffusion parameters except for the spin speed were identical. In addition to the spin speed, also the diffusion temperature has an influence on the uniformity of the sheet resistance. At increased diffusion temperature, a more uniform sheet resistance is obtained. However, at temperatures above 600 $^{\circ}\text{C}$, the SOD is more sensitive to crack formation and additionally germanium oxide is formed more easily, so preferably the diffusion temperature is taken in the range of 550 to 600 $^{\circ}\text{C}$.

Table II: Overview of 4-point probe resistivity measurements illustrating the uniformity of the phosphorous doping profile over the sample area (17 data points, 19.6 cm^2).

SOD-type	Spin speed (rpm)	R_s ($\Omega\text{m}/\text{sq.}$)	Dev. ($\Omega\text{m}/\text{sq.}$)
P506, 1% P	4000	54.6	11.0
P506, 1% P	3000	38.2	2.0

2.2 Back contact formation

During the second step of the solar cell process (Table I, step 2), the back contact is realised by Al evaporation. To create a back-surface field (BSF), the

sample is annealed above the eutectic temperature (426 $^{\circ}\text{C}$), such that a compound consisting of Al and Ge is obtained. In germanium, Al has a relatively high maximum solid solubility of $2 \cdot 10^{20} \text{ cm}^{-3}$, such that the BSF can be very effective. An estimate of the surface recombination velocity obtained on realised solar cells is made by simulation of the measured quantum efficiency curves using the software tool PC-1D [4]. The value of the surface recombination velocity of the realised BSF is in the order of 100 to 200 cm/s for a substrate with a doping level of $3 \cdot 10^{15} \text{ cm}^{-3}$. In the recently realised solar cells this value will be slightly higher due to the higher doping level of the substrate.

A disadvantage of this type of backside contact is its relatively low reflectivity. Due to the fact that at the interface a eutectic is formed between Al and Ge, the surface is rough and the reflection, as measured at the front, is limited to 20 percent at a wavelength of 1800 nm. To improve the optical confinement an alternative back side contact structure is under investigation [5].

2.3 Surface passivation

After definition of the cell area by wet chemical etching (Table I, step 3), the front surface is passivated by amorphous silicon deposited using plasma enhanced chemical vapour deposition (PECVD) (Table I, step 4). To obtain high quality surface passivation, the surface preparation method is of utmost importance. Besides the removal of the highly doped surface area, it is critical that all the germanium oxide present on the surface is effectively removed before the amorphous silicon layer is deposited. This germanium oxide layer is formed both by native growth in air and by application of the wet-chemical cleaning steps containing oxidising chemicals like H_2O_2 . In addition to the surface pre-treatment, important parameters are the deposition temperature, plasma power and layer thickness. On lowly doped substrates ($2 \cdot 10^{14} \text{ cm}^{-3}$) a surface recombination velocity of 20 cm/s has been measured [6].

In solar cell processing it is observed that the thickness of the amorphous silicon layer is first of all of importance with respect to the quality of passivation. A layer of a-Si thinner than 30 nm, results in a higher surface recombination velocity compared to a layer with a thickness of 30 to 60 nm [6]. A layer thickness of over 100 nm should be avoided in order to minimise the optical losses (application under the AM1.5 spectrum). Furthermore, the thickness of the layer is important with respect to the contact formation, since a too thick layer will hinder the creation of a conducting path through the amorphous silicon layer, as will be further discussed in the next section.

Besides the nominal thickness of the amorphous silicon layer also its uniformity is important, especially with respect to the contact formation process. For an amorphous silicon layer with an average thickness of 40 nm, as measured by a Gaertner L116B ellipsometer, the deviation over the sample area is in the range of 6 to 8 percent. Such variations in layer thickness are acceptable with respect to the contact formation process.

2.4 Front contact formation

As a consequence of the use of amorphous silicon for germanium surface passivation, the processing possibilities with respect to front contact formation are

restricted (Table I, step 5). Three different methods as shown in Figure 2 have been investigated.

The first method to realise the front contact consists of two steps, the formation of the Ohmic contact followed by the deposition of the passivation layer. A disadvantage of this method is that the quality of the surface passivation is limited by the restrictions in surface cleaning imposed by the metal contact. The resulting lack of quality of the surface passivation has limited the maximum efficiency of solar cells realised with this method to 4 percent (AM1.5G).

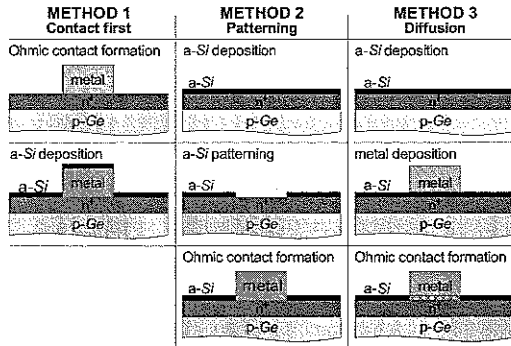


Figure 2: Overview of three possible front contact formation methods namely, contact first, patterning and diffusion.

The second method is the most common, as often used for silicon devices, where the passivation layer is patterned such that the subsequently deposited contacting metal is in direct contact with the emitter. In case of germanium, selective patterning of the a-Si layer is not straightforward due to the lack of wet or dry amorphous silicon etch processes with a sufficiently high selectivity with respect to germanium. Especially using a wet-chemical etching method resulted in non-uniform etching over the wafer area. Using a non-optimised dry RIE/ICP etching process has resulted in solar cell fill factors of 62 percent for cells with a relatively low V_{oc} of 220 mV using Ti/Pd/Ag contacts.

The third method is the most innovative and has been studied in more detail. Here, the metal is diffused through the passivation layer to make contact with the emitter. Important are the specific properties of the diffusing metal, diffusion temperature, diffusion time and furthermore the thickness of the amorphous silicon layer. The best front contact is obtained by application of a double metal layer consisting of Pd and Ag. Palladium is used to obtain fast diffusion through the amorphous silicon layer [7] and at the same time get limited diffusion in germanium. The additional layer of Ag is needed to lower the series resistance. Application of this double-metal layer as the front metal of a germanium solar cell has resulted in a best solar cell fill factor of 68.5 percent for a cell with a V_{oc} of 255 mV. Note that, taken into account the dependence of the fill factor on the V_{oc} , this FF is very close to its maximum value of 69.0 percent. In this case an optimised finger pattern has been used, designed to be applied under the AM1.5G spectrum.

Annealing of the Pd/Ag contact is done at temperatures between 200 and 250 °C. In this temperature range the contact formation is influenced by

several processes. First of all, silicide (Pd_2Si) formation occurs in the amorphous silicon layer at temperatures of 100° to 300 °C and similarly germanide ($PdGe$, Pd_2Ge) formation occurs at the germanium surface when using temperatures above 230 °C [8, 9]. Furthermore, local palladium induced crystallisation of the amorphous silicon layer might occur, depending on the temperature, the palladium content, the amount of defects in the a-Si layer and the contact formation time [10]. Induced crystallisation can be of influence, since the maximum solid solubility of Pd in c-Si is limited to values below $1 \cdot 10^{15} \text{ cm}^{-3}$ for low temperatures.

A preliminary indication of palladium induced crystallisation has been obtained while varying the amorphous silicon layer thickness. For a certain a-Si layer thickness, it is found that no longer a contact can be realised at a relatively low temperature even for increased diffusion time. However, applying a slightly higher diffusion temperature results in a good contact with excellent solar cell fill factors. Further research will be needed to find the exact cause of this phenomenon.

Depending on the thickness of the amorphous silicon layer, for a given annealing temperature, a clear evolution of the solar cell fill factor is observed as a function of annealing time. This behaviour is illustrated in Figure 3, where the IV-curve of a germanium solar cell is given as function of annealing time. Annealing for an even longer period of time results in a slight decrease in series resistance, however simultaneously a decrease in shunt resistance leading to gradual shunting of the solar cell is observed.

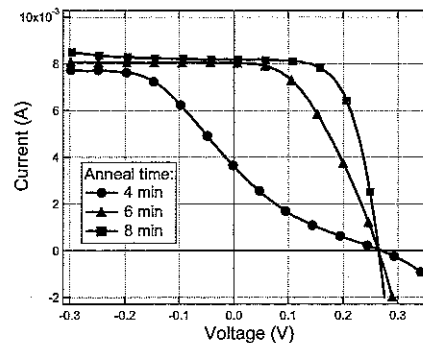


Figure 3: Illustration of the evolution of the IV-curve of a germanium solar cell, as a function of annealing time of the front side contact consisting of Pd/Ag.

3 SOLAR CELL RESULTS

As a result of the detailed study of the different aspects of the germanium solar cell process, significant improvement of the germanium solar cell properties has been achieved recently.

In this work the realised germanium solar cells have been analysed using the AM1.5G spectrum. To assess the quality of the realised solar cells, simulated (PC-1D) cell parameters are shown in the first row of Table III for comparison. Assuming a front and back surface recombination velocity of $1 \cdot 10^4$ and $1 \cdot 10^3$ cm/s respectively, an emitter sheet resistance of 50 Ohm/square and realistic optical losses results in a simulated energy conversion efficiency of 9.6 percent.

Table III: Overview of realised germanium solar cell parameters (AM1.5G, C=1 sun), as measured at IMEC. For comparison simulated data is given.

	J_{sc} (mA/cm ²)	V_{oc} (%)	FF (%)	Eff (%)
Simulation	50.0	273	70	9.6
Previous cell [2]	45.6	245	59.6	6.7
Best 1×1 cm ²	47.8	255	66.4	8.1
Best 0.5×0.5 cm ²	50.2	257.7	64.8	8.4

The developed germanium solar cell process has resulted in world-class energy conversion efficiencies well above 7 percent (AM1.5, C=1 sun). Today, our best realised 1×1 cm² germanium solar cell has an AM1.5G efficiency of 8.1 percent, as shown in Table III. Furthermore a 0.5×0.5 cm² cell has been realised with a record efficiency of 8.4 percent, with a J_{sc} of 50 mA/cm², a V_{oc} of 258 mV and a FF of 65 percent. This cell has been separated from other cells by dicing using a diamond wafer dicer. The IV-curves of these cells are shown in Figure 4. The data and IV-curve of a germanium solar cell realised previously [2] is given for comparison. The applied anti-reflective coating consists of a double layer of ZnS and MgF₂, optimised for the AM1.5G spectrum.

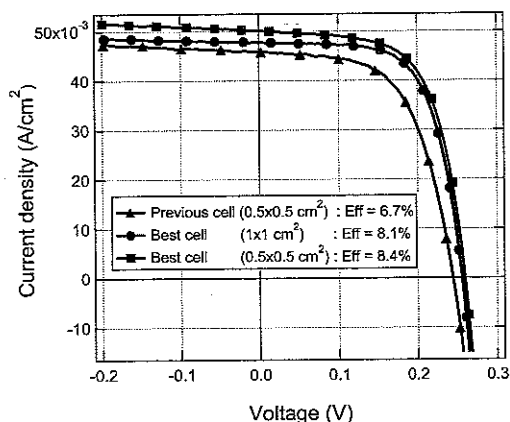


Figure 4: Measured IV-curves (AM1.5G, C=1 sun) of the recently realised germanium stand-alone solar cells, compared to the IV-curve previously presented [2].

Compared to the simulated solar cell data, our cells show an excellent current density. There is still room for improvement on the level of the V_{oc} , which can be further optimised by lowering the surface doping level in order to obtain a lower surface recombination velocity. Additionally the FF can be further increased by an in-depth study of the contact formation process. With further optimisation stand-alone germanium solar cell efficiencies of 9 to 9.5 percent should be feasible.

4 CONCLUSIONS

A process has been developed to realise a germanium stand-alone solar cell. Such a stand-alone germanium solar cell can be applied in various systems like mechanically stacked high-efficiency multi-junction solar cells, thermo-photovoltaic systems or hybrid lighting systems. The various steps needed in this

process, namely emitter formation, surface passivation and the formation of front and rear contacts, have been studied in detail. Optimisation of the process has resulted in a best world-class solar cell energy conversion efficiency of 8.4 percent (AM1.5G, C=1 sun).

Application of the realised germanium solar cell in a mechanically stacked high-efficiency solar cell, theoretically can result in a total efficiency of around 34 percent (AM1.5, C=1 sun), assuming no optical losses, where the germanium cell contributes with an efficiency of 3.9 percent.

Further research will be focused on improvement of the V_{oc} and FF. Besides additional optimisation of the cell process, reliability tests will be done to assess the behaviour of the solar cells on longer term. In this frame, temperature cycling and temperature storage tests will be performed in the near future.

ACKNOWLEDGEMENTS

The cells were measured against a reference cell which is calibrated (traceable) to the World Radiometric Reference by the European Solar Test Installation (ESTI) of the European Commission Joint Research Centre, an ISO 17025 accredited calibration laboratory.

REFERENCES

- [1] N.E. Posthuma, G. Flamand and J. Poortmans, patent US2005000566 (2005).
- [2] N.E. Posthuma, G. Flamand and J. Poortmans, 'Development of stand-alone germanium solar cells for application in space using spin-on diffusants', Proceedings of 3rd World Conference on Photovoltaic Energy Conversion, 11-18 May 2003, Osaka, Japan, Vol. 1, 777-780 (2003).
- [3] N.E. Posthuma, J. van der Heide, G. Flamand and J. Poortmans, 'Emitter formation and contact realization by diffusion for germanium photovoltaic devices', submitted for publication in IEEE Transactions on electron devices (2006).
- [4] P.A. Basore and D.A. Clugston, PC1D, University of New South Wales Version 5.6 (2001).
- [5] J. van der Heide, N.E. Posthuma, G. Flamand and J. Poortmans, 'Improving the backsurface reflection of germanium thermophotovoltaic cells using laser fired contacts', presented at 21st EPVSEC Dresden 2006, paper 1AO.7.3.
- [6] N.E. Posthuma, G. Flamand, W. Geens and J. Poortmans, 'Surface passivation for germanium photovoltaic cells', Solar Energy Materials and Solar Cells, Vol. 88(1), 37 (2005).
- [7] S. Coffa, et al., 'Determination of diffusion mechanisms in amorphous silicon', Physical review B, Vol. 45 (15), 8355-8358 (1992).
- [8] E.D. Marshall, et al., 'Metal-germanium contacts and germanide formation', Mat. Res. Soc. Symp. Proc. 47, 161166 (1985).
- [9] F. Edelman, et al., 'Interfacial reactions in the Pd/a-Si/c-Si system', Journal of applied physics, Vol. 71(1), 289-295, (1992).
- [10] S. Lee, B. Lee, T. Kim and S. Joo, 'Pd₂Si-assisted crystallisation of amorphous silicon thin films at low temperature', Journal of applied physics, Vol. 85(10), 7180-7184 (1999).